

Cite this: *Chem. Sci.*, 2023, 14, 6730

All publication charges for this article have been paid for by the Royal Society of Chemistry

Received 2nd May 2023

Accepted 25th May 2023

DOI: 10.1039/d3sc02253f

rsc.li/chemical-science

# The contrasting reactivity of *trans*- vs. *cis*-azobenzenes (ArN=NAr) with benzynes†

Dorian S. Sneddon and Thomas R. Hoye \*

We report here a study that has revealed two distinct modes of reactivity of azobenzene derivatives (ArN=NAr) with benzynes, depending on whether the aryne reacts with a *trans*- or a *cis*-azobenzene geometric isomer. Under thermal conditions, *trans*-azobenzenes engage benzyne via an initial [2 + 2] trapping event, a process analogous to known reactions of benzynes with diarylimines (ArC=NAr). This is followed by an electrocyclic ring opening/closing sequence to furnish dihydrophenazine derivatives, subjects of contemporary interest in other fields (e.g., electronic and photonic materials). In contrast, when the benzyne is attacked by a *cis*-azobenzene, formation of aminocarbazole derivatives occurs via an alternative, net (3 + 2) pathway. We have explored these complementary orthogonal processes both experimentally and computationally.

## 1 Introduction

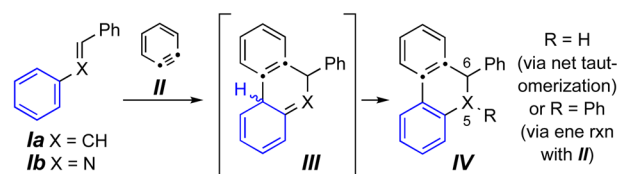
Benzynes (and arynes more generally) are remarkably versatile reactive intermediates, especially with respect to the manifold classes of trapping agents with which they will engage.<sup>1</sup> Azoarenes (ArN=NAr) comprise a class of compounds of long-standing interest.<sup>2</sup> We can locate only a single report of reactions of azo compounds with benzynes.<sup>3</sup> In that work products containing an *N*-aminocarbazole skeleton were produced. We describe here a detailed investigation into the complementary modes of reactivity observed between benzynes and *trans*- vs. *cis*-azobenzenes.

Reactions of benzynes with the related trapping agents stilbenes<sup>4,5</sup> (**1a**) and its mono aza-analog *N*-benzylideneaniline<sup>6,7</sup> (**1b**) are known (Fig. 1a). With classically generated benzynes [e.g., *o*-benzyne (**II**)] these proceed by either exclusive or predominant formation of initial [4 + 2] cycloadducts (cf. **III**), which then tautomerize to products **IV**. In contrast, imines such as **1b** engage the more complex and, necessarily, sterically hindered hexadehydro-Diels–Alder (HDDA) benzynes **V**, to give dihydroacridines **VIII** arising from an initial [2 + 2] event (cf. **VI**) and ensuing electrocyclic ring-opening (cf. **VII**) and -closing processes (Fig. 1b).<sup>8</sup>

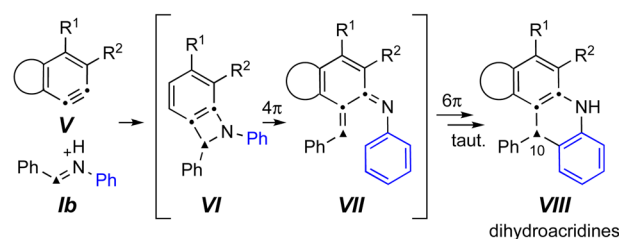
The sole example we can locate of diaza-analogs of stilbenes – i.e., azoarenes (**IX**) – engaging *o*-benzynes was recently described by Wang, Li, and coworkers and proceeded via a net (3 + 2) cycloaddition under sunlight (Fig. 1c).<sup>3</sup> This produced the *N*-aminocarbazole derivatives **XI**, a process suggested to take place via zwitterionic intermediates **X**. The authors noted that

in the absence of sunlight the same “reaction did not proceed.”<sup>3</sup> This led us to question which of the three distinct modes of reaction shown in Fig. 1 would ensue when an azobenzene engaged a (more hindered) “HDDA benzyne.” Would an overall [4 + 2] pathway lead to a dihydrocinnoline skeleton (a 5,6-diaza-

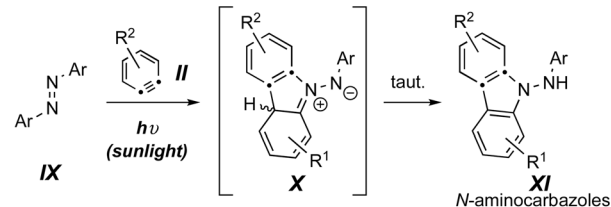
### a stilbenes (X = CH) and diarylimines (X = N) with “classical benzynes”: [4+2]



### b diarylimines with “HDDA benzynes”: [2+2]



### c azoarenes with “classical benzynes”: (3+2)



Department of Chemistry, University of Minnesota, 207 Pleasant St. SE, Minneapolis, MN 55455, USA. E-mail: hoye@umn.edu

† Electronic supplementary information (ESI) available. CCDC 2251646 and 2251645. For ESI and crystallographic data in CIF or other electronic format see DOI: <https://doi.org/10.1039/d3sc02253f>

Fig. 1 (a) Known reactions of classical benzynes with stilbenes and imines. (b) Known reactions of imines with HDDA-benzynes.<sup>8</sup> (c) Known photo-stimulated reactions of azoarenes with benzynes.<sup>3</sup>



analog of **IV**); would an initial [2 + 2] pathway produce a dihydrophenazine (a 10-aza analog of **VIII**); or would the reaction mirror the case of the photochemically driven process to give *N*-aminocarbazoles analogous to **XI** as observed by Li *et al.*?<sup>3</sup>

## 2 Results and discussion

We elected to start our investigations by using a prototypical thermal HDDA substrate. In one of our earliest experiments

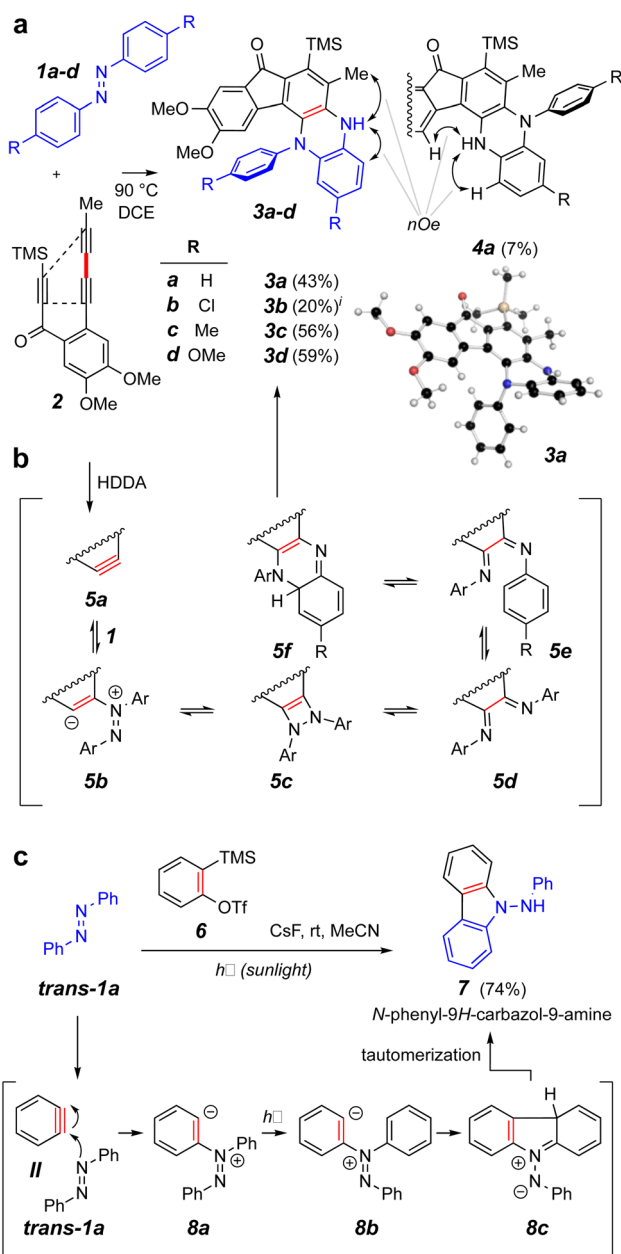


Fig. 2 (a) Reaction of *trans*-azobenzene derivatives **1a–d** with the benzyne produced by heating triyne **2** to give dihydrophenazines **3** and **4**. (b) Possible intermediates on the reaction coordinate leading to the dihydrophenazines. (c) Contrasting mode of reactivity when *o*-benzyne (**II**) engages azobenzene (**trans-1a**) during exposure to sunlight.<sup>3</sup> <sup>†</sup>A small amount of the analog of isomer **4a** was observed in the chromatographed sample of this product (see ESI<sup>†</sup>).

(Fig. 2a), *trans*-azobenzene (**trans-1a** = **IX**, 10 equiv.) and the triyne **2** were heated together in a solution of 1,2-dichloroethane (DCE) at 90 °C for 15 h. This is a temperature at which **2** will undergo a HDDA cycloisomerization<sup>9</sup> to give the corresponding benzyne (*cf.* **5a**, Fig. 2b). This experiment produced the mono-arylated dihydrophenazine **3a** along with a small amount of its regioisomeric product **4a** in modest yields. The structures of these isomers were definitively distinguished by the complementary, indicated nOe interactions involving the NH proton in each. This structure assignment was further substantiated by an X-ray diffraction analysis of the major isomer **3a**. Notably, the pathway leading to the phenazine skeleton in **3a** is new and distinct from that observed in the reported photo-induced reactions leading to aminocarbazole derivatives (Fig. 1c). Likewise, the additional azobenzene derivatives **1b–d** gave the dihydrophenazines **3b–d** as the major if not solely observed products.

The formation of products having the phenazine skeleton from the reaction of an aryne and an azobenzene is novel. Phenazines and dihydrophenazines are of considerable current interest.<sup>10</sup> For example, they are important in the arenas of optical sensing, electrochemistry, and organic electronics and photonics.<sup>11</sup> In the optical sensing realm, these can show vibration-induced emission (VIE), allowing them to exhibit multicolor emission. Additionally, certain phenazines exhibit thermally activated delayed fluorescence (TADF), making them attractive organic light-emitting diode (OLED) candidates. Phenazine derivatives may additionally act as ion battery cathode materials. They can also be incorporated into various organic frameworks for use as both electronic and photonic materials. Also, phenazines and dihydrophenazines are commonly found as secondary metabolites, some of which also have interesting biological properties.<sup>12,13</sup>

A mechanistic possibility for the outcome of the thermal reactions with *trans*-azobenzenes leading to the phenazine skeleton is suggested by structures **5a–f** (Fig. 2b). This is discussed in greater detail in conjunction with the DFT studies shown in Fig. 3. A contrasting mechanistic rationale for the aminocarbazole formation seen in the work of Wang *et al.* is shown in Fig. 2c. They proposed that the generation of *o*-benzyne (**II**) by the Kobayashi method in the presence of *trans*-azobenzene (**trans-1a**) gave rise by nucleophilic attack to the zwitterion **8a** and that this species absorbed a photon that resulted in isomerization to its geometric isomer **8b**. This then cyclized to form the new five-membered ring present in the species **8c** (aza-Nazarov-like), a tautomer of the more stable, aromatized aminocarbazole **7**.

We turned to DFT studies to parse out some of the energetic details associated with these contrasting modes of reaction. A full potential energy surface (PES) for the pathway leading to the dihydrophenazine is shown in Fig. 3a. *trans*-Azobenzene (**trans-1a**) engages *o*-benzyne via **TS1** to form zwitterion **trans-9b** (= **8a**, Fig. 2c). We computed this zwitterion to undergo transformation to either the benzodiazetidine **trans-9c** via **TS3** or to the zwitterion **9a** (= **8c**, Fig. 2c) via **TS2**. The very similar energies of activation for these competing processes is inconsistent with the fact that we did not observe any products with the

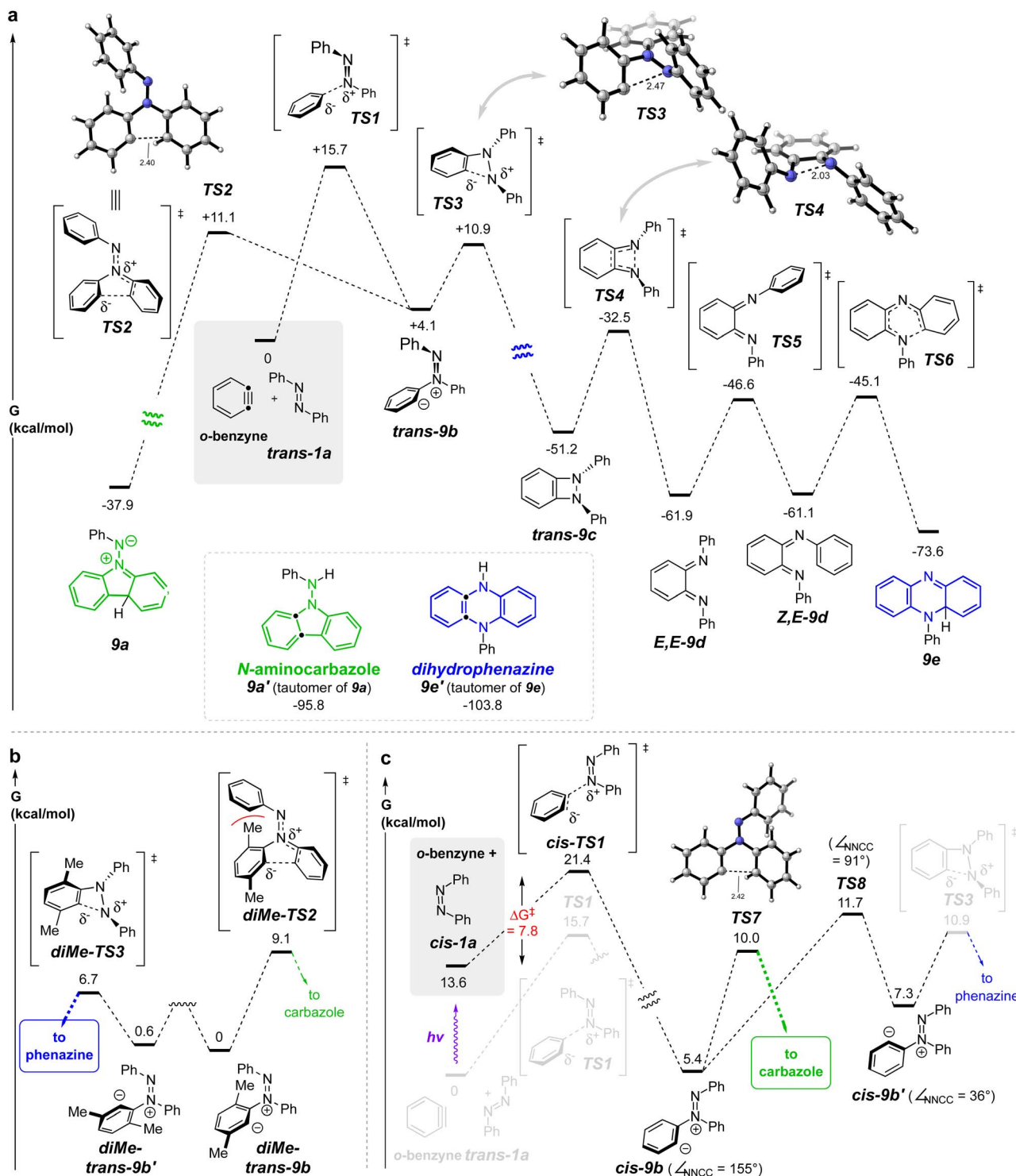


Fig. 3 (a) DFT<sup>†</sup> potential energy surface for the reaction of *o*-benzyne with *trans*-azobenzene (*trans*-1a) (gray box) leads to both phenazine and carbazole skeletons with essentially the same activation barrier (cf. TS2 vs. TS3). (b) The more hindered 3,6-dimethylbenzyne, a better mimic of an HDDA-benzyne, shows a significant preference for the phenazine-forming pathway (cf. *diMe*-TS3 vs. *diMe*-TS2). (c) *cis*-Azobenzene (*cis*-1a) gives *cis*-9b, the precursor to the carbazole product, via a lower activation barrier (7.8 kcal mol<sup>-1</sup>) than that of *trans*-1a to TS1 (15.7 kcal mol<sup>-1</sup>), the forerunner to the phenazine product; *cis*-9b proceeds to the aminocarbazole product via TS7 faster than isomerizing to *cis*-9b', which could have led to the dihydrophenazine product via TS3. <sup>†</sup>SMD(benzene)/MN15/6-311++G(d,p).

aminocarbazole skeleton in the HDDA reactions described in Fig. 2a, an important point to which we return in the following paragraph. The benzodiazetidine *trans*-9c is a rare type of

intermediate. The only compound we can find containing a benzodiazetidine (7,8-diazabicyclo[4.2.0]octa-1(6),2,4-triene) substructure is that of the parent, fully unsubstituted

molecule, formed in an argon matrix and characterized by its infrared spectroscopic features.<sup>14,15</sup> This transient species rapidly ring-opened to the bis-imino-*o*-benzoquinone. Likewise, **trans-9c** was computed to isomerize to the bis-imine **E,E-9d** through a conrotatory electrocyclic ring opening *via* **TS4**. *E/Z*-Isomerization *via* **TS5** (N-inversion) give the diiminoquinone **Z,E-9d**, which is poised to undergo  $6\pi$ -electrocyclization *via* **TS6** to furnish the penultimate intermediate **9e**. Notably, all of the activation barriers (*via* **TS1–TS6**) on this computed potential energy surface are  $<20$  kcal mol<sup>−1</sup>.

Recall that the barrier for the cyclization of **trans-9b** to a five-membered ring (aza-Nazarov) enroute to **9a** was essentially identical with that leading to the diazetidine **trans-9c**. Why, therefore, did we not see aminocarbazole formation in the reactions of the HDDA-benzynes with *trans*-azobenzenes **1a–d**? The HDDA benzyne bears substituents on carbons 3 and 6 flanking the sp-hybridized benzyne carbons. To assess the impact of this type of substitution, we computed the analogous key intermediates for reaction between **trans-1a** and, now, 3,6-dimethyl-*o*-benzyne (Fig. 3b). A striking preference ( $\Delta\Delta G^\ddagger = 2.4$  kcal mol<sup>−1</sup>) for cyclization to the benzodiazetidine was seen. This difference is attributable to the unfavorable steric interaction portrayed in **diMe-TS2** when compared to that in **diMe-TS2**. The explicit precursors to these two transition structures are the conformers **diMe-trans-9b** and **diMe-trans-9b'**, respectively; related conformers will play a role in later discussion of formation of aminocarbazole products.

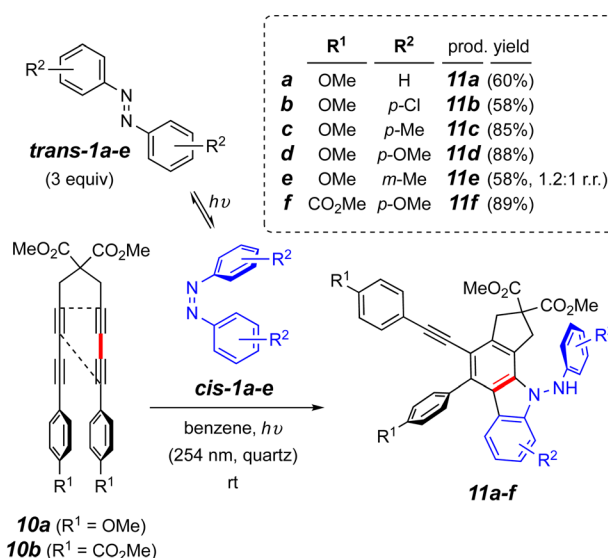
The formation of dihydrophenazine derivatives by this unprecedented process is appealing, and we were encouraged to explore potential improvements in the efficiency of the transformation. In turn, this led us to consider modifications that might improve this process. The barrier of 15.7 kcal mol<sup>−1</sup> for **trans-1a** to traverse **TS1** is higher than a number of other additions to arynes by species containing nucleophilic nitrogen atoms.<sup>16–18</sup> We speculated that *cis*-azobenzene (**cis-1a**), having easier steric access to each azo nitrogen atom as well as greater negative charge character at each of its nitrogens [*e.g.*, atomic polar tensor =  $-0.167$  vs.  $+0.008$  for *cis*- vs. *trans*-azobenzene, respectively (APT in Gaussian)] could serve as a more competent nucleophile in this process. *cis*-Azoarenes have been reported to engage in net-cycloaddition reactions faster than their *trans*-counterparts.<sup>19–23</sup>

The computed PES for the reaction between **cis-1a** and *o*-benzyne is shown in Fig. 3c. Significantly, the activation barrier passing through **cis-TS1** enroute (to **cis-9b**) is computed to be nearly 8 kcal mol<sup>−1</sup> lower than that for **trans-1a** to proceed through **TS1** (to **trans-9b**): *i.e.*, 7.8 vs. 15.7 kcal mol<sup>−1</sup>. This led us to first investigate whether we could use photons to produce a sufficiently high proportion of **cis-1a** to allow the overall energetically favored process to be the capture of the benzyne by the *cis*-azobenzene. (Later we return to discuss the remainder of the computed energetics shown in Fig. 3c proceeding onward from **cis-9b**).

To address this question, we carried out the first experiment shown in Fig. 4a. This involved use of the tetrayne **10a**, an HDDA substrate known to efficiently undergo photo-induced cycloisomerization to its corresponding HDDA-benzyne.<sup>24</sup> This

allowed both of the benzyne and *cis*-azobenzene reactants to be formed at ambient temperature when irradiated at 254 nm. We pre-irradiated **trans-1a** in benzene in a quartz vessel in a Rayonet reactor for 1 h. Tetrayne **10a** was introduced and irradiation continued overnight. This resulted in a single isolable product that, to our surprise proved not to be the expected dihydrophenazine analog of **3a**. Instead, this was deduced to be the aminocarbazole compound **11a**. This process was shown to be general, proceeding also starting with the azobenzenes **trans-1b–e**. Those with more electron rich aryl substituents resulted in higher product yields. The ester-substituted tetrayne **10b** also showed very efficient conversion to product **11f**. The structure assignments of this series of products was reflected in their parallel NMR spectral properties, as seen from extensive interpretation of both 1D as well as 2D <sup>1</sup>H and <sup>13</sup>C spectra. In addition, an X-ray diffraction structure of the analog **11b** confirmed the assignments of these aminocarbazole-containing compounds (Fig. 4b).

#### a engagement of photochemical HDDA benzynes with *cis*-1a–e



#### b single-crystal X-ray diffraction structure of **11b**

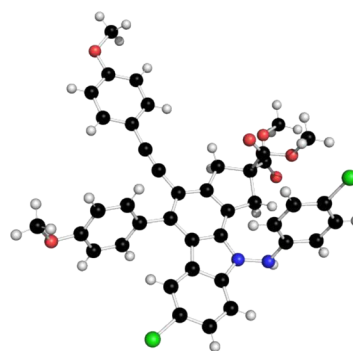


Fig. 4 (a) Reaction of photochemical HDDA precursors **10a–b** with a photo-generated mixture of *trans*- and *cis*-**1a–f** under continuous irradiation; (b) single-crystal X-ray diffraction structure of **11b**.





To probe the involvement of the *cis*-azobenzene in benzyne trapping more explicitly, we explored the trapping of a "Kobayashi-generated benzyne"<sup>25,26</sup> as presented in Fig. 5. When *o*-benzyne was generated from 2-trimethylsilylphenyl triflate (**6**) starting with 3 equivalents of a preirradiated solution of a *trans*-azobenzene derivative and under further continuous irradiation, the photochemically established amount of the *cis*-azobenzene **cis-1a**, **cis-1c**, or **cis-1d** proceeded to give the respective aminocarbazole derivative **7a**, **7c**, or **7d** in good yield (Fig. 5a). As further evidence that the *cis*-azobenzene geometric isomer is the key reactive intermediate effecting each of these overall transformations, **cis-1a** was purified by flash chromatography and used soon thereafter as a single isomer to trap *o*-benzyne (Fig. 5b). In an experiment employing only 1.1 equivalent of pure **cis-1a** relative to the Kobayashi precursor **6**, the aminocarbazole **7a** was obtained in similar yield to that arising from the photostationary mixture of the azobenzenes. Finally, generating *o*-benzyne in the presence of pure **trans-1a** (1.1 equivalent) but in the absence of irradiation gave no discernible amount of the aminocarbazole derivative **7a**. The yield of this reaction was not as high as for the more hindered HDDA benzynes, perhaps because of some competing secondary reaction between the NH<sub>2</sub> group in **7a** and additional *o*-benzyne. Collectively, the computational and experimental results

presented in Fig. 3–5 indicate that (i) the *cis*-azobenzene geometric isomer is a more reactive trap for a benzyne, (ii) *cis*-azobenzene is the key intermediate responsible for launching the transformation leading to aminocarbazole derivatives, and (iii) the *trans*-azobenzene geometric isomer is uniquely responsible for furnishing dihydrophenazines in the case of HDDA benzynes. In view of these results, we suggest that the process leading to aminocarbazole formation is better viewed as arising from the innate reactivity of *cis*-azobenzene itself (*cf.* Fig. 3c) rather than one in which intermediate **trans-9b** is photoisomerized to **cis-9b** (*cf.* **8a** to **8b**, Fig. 2c).<sup>3</sup>

Having clearly demonstrated experimentally that the *cis*-azobenzene isomer is responsible for redirecting the mode of reaction with benzynes to produce aminocarbazoles rather than dihydrophenazines, we further explored the behavior of the zwitterion **cis-9b** by DFT (Fig. 3c). This species can either undergo aza-Nazarov cyclization directly to the carbazole skeleton *via* **TS7** or undergo an aryl rocking motion (**TS8**) to access an alternative rotamer of the zwitterion, namely **cis-9b'**. While **cis-9b'** could geometrically access **TS3**, thereby intersecting with the phenazine pathway, we found, perhaps somewhat surprisingly, that the rotational barrier to produce **cis-9b'** *via* **TS8** was higher than proceeding to the aminocarbazole *via* **TS7** by 1.7 kcal mol<sup>−1</sup>. We attribute the relatively high barrier of aryl rotation to the penalty of breaking conjugation of the 1,2-diazabuta-1,3-butadiene system in the nearly orthogonal transition state geometry (*cf.* dihedral angle values in **cis-9b** and **cis-9b'** vs. **TS8**). Taken at face value, these energetics suggest that *ca.* 95% of **cis-9b** should undergo aza-Nazarov cyclization to the carbazole rather than isomerizing to **cis-9b'** and furnishing phenazine products.

Likewise, we explored by DFT (see Fig. S7 in the ESI† for details) whether **cis-9b** could isomerize directly to **trans-9b** (and then on to the phenazine) by the net isomerization of the N=N double bond geometry. This could occur either (i) by linearization of the N=NPh geometry (*i.e.*, inversion *via* an sp<sup>2</sup>-hybridized nitrogen, *cf.* **TS5**, Fig. 3a) or (ii) by out-of-plane rotation about the N=N bond. A TS for the former process was located and it showed a free energy >20 kcal mol<sup>−1</sup> higher than that of **TS7**. Attempts to find a TS for the latter geometric change instead optimized directly to **TS3**. These results suggest that it is unlikely for **cis-9b** to give rise to **trans-9b**, thereby precluding a second pathway by which the zwitterion **cis-9b** could give rise to a product having a phenazine skeleton.

To gain evidence addressing the later stages of the thermal mechanism involving the interesting electrocyclic processes emanating from the benzodiazetidione **trans-9c** (identified by the computations summarized in Fig. 3a), we synthesized the phenanthrene-diiminoquinone **12**. In particular, we thought that the thermal behavior of this compound, an analog of species **E,E-9d** in the computational study, would shed light on the remaining steps in the mechanism (*i.e.*, isomerization to **Z,E-9d** and its electrocyclic closure to the 4a,5-dihydrophenazine **9e**). The first hint of some unusual behavior of species **12** arose while attempting its preparation following a literature protocol for TiCl<sub>4</sub>-promoted condensation of 9,10-phenanthrenequinone with anilines.<sup>27,28</sup> In our hands this

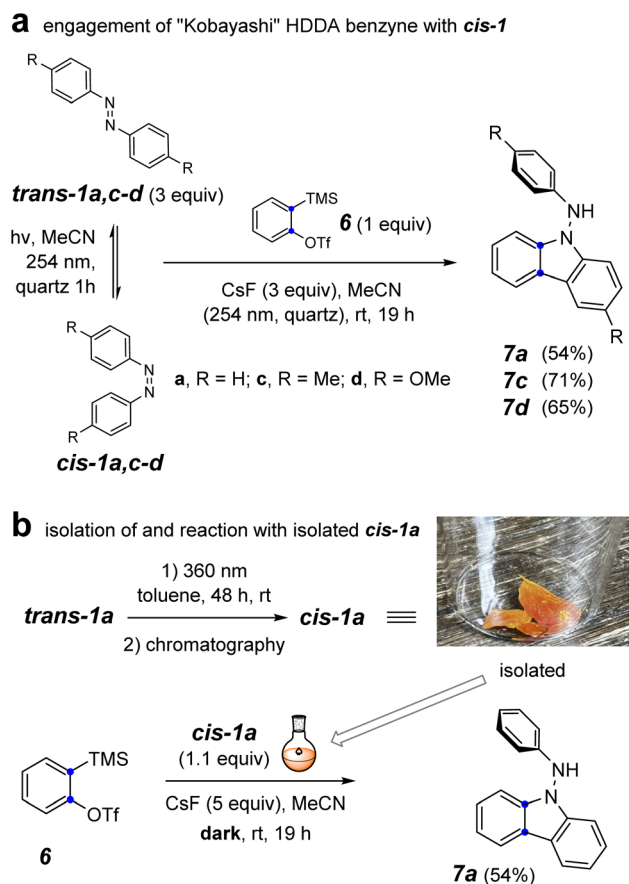


Fig. 5 Reaction of *o*-benzyne with (a) a photo-generated mixture of *trans*- and *cis*-**1a,c-d** under continuous irradiation and (b) isolated *cis*-**1a** in the dark.

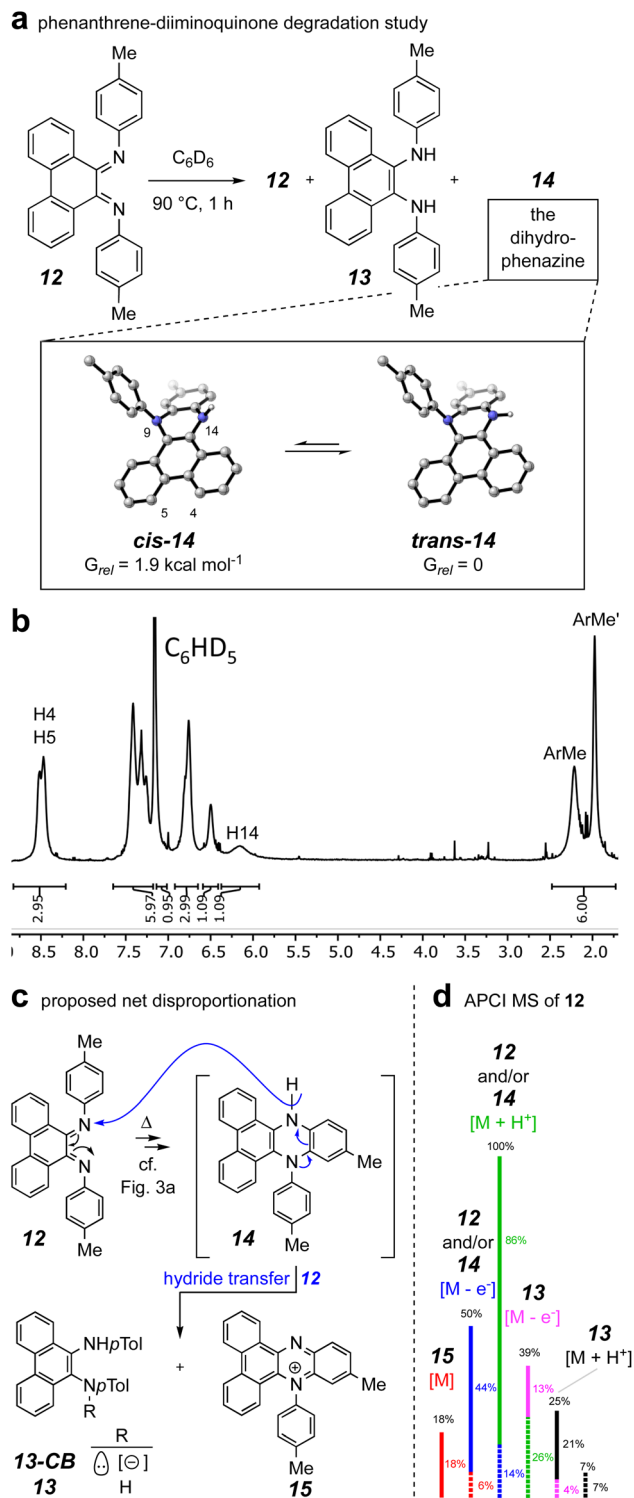


Fig. 6 Disproportionation processes emanating from the diiminoquinone **12** to produce the diamine **13** and the phenazinium ion **15** via the dihydrophenazine **14**. (a) The reaction taken to partial conversion from which **14** was isolated along with a coeluting mixture of starting material (**12**) and **13**. (b)  $^1\text{H}$  NMR spectrum of **14**. (c) A mechanistic rationale for the overall redox-neutral transformation. (d) Illustration of the mixture of species/ions formed while recording an APCI mass spectrum of an isolated sample of the diiminoquinone **12**.

repeatedly gave a complex array of products from which the major isolable product was, surprisingly, the diamine **13**. Once in hand, this could be smoothly oxidized to **12** using  $\text{MnO}_2$ , although its disproportionation lability upon further handling was soon recognized.

When **12** was warmed in deuterobenzene ( $90\text{ }^\circ\text{C}$ ), its transformation could be monitored by  $^1\text{H}$  NMR spectroscopy. An experiment that was terminated after 1 h (ca. 67% conversion of the starting **12**) resulted in generation of a mixture of the diamine **13** and dihydrophenazine **14** (Fig. 6a) in addition to the unreacted **12**. Chromatographic purification provided a pure sample of the dihydrophenazine **14**, which proved to be even more labile than its isomer **12**. The  $^1\text{H}$  NMR spectrum of **14** (Fig. 6b) contained broad resonances; in retrospect these were also seen in the spectrum of the reaction mixture itself (see Fig. S4†). We identified by DFT two nearly equienergetic, diastereomeric, *cis*- and *trans*-conformers of **14** that differ only in the relative orientation of the hydrogen atom and lone pair of electrons on N14. The NMR spectrum of a *N5,N10*-diarylated analog having the same dibenzodihydrophenazine skeleton as **14** showed similar broadening.<sup>29</sup> This spectroscopic phenomenon, along with the lability we observed for **14**, could explain why past researchers have not recognized that *N,N*-diaryl-9,10-diiminophenanthrenequinones such as **12** undergo a facile  $6\pi$ -electrocyclization.<sup>27</sup>

The presence of the diamine **13** arising from the condensation reaction meant to provide **12** (see ESI† for details) and the degradation behavior of **14** were initially puzzling; they implied that redox events were occurring. The only material present in the crude mixture that would serve as a reasonable reductant was the dihydrophenazine **14**. Thus, we envisaged (Fig. 6c) an overall net disproportionation sequence in which formation of **14** (cf. mechanism delineated in Fig. 3a) sets up reduction of a second equivalent of **12** via hydride transfer to give the phenazinium cation **15** and the conjugate base of **13** (**13-CB**) as its counter anion. A stylized APCI mass spectrum of a sample of purified diiminoquinone **12**, ionized by thermal activation, is shown in Fig. 6d. Evidence for all of species **12**–**15** can be seen in the data. Taking into account the proportion of natural abundance  $^{13}\text{C}$  isotopologues for each member of this array of  $\text{C}_{28}$  species (dashed lines) allows deconvolution of the entire set of ion intensities as indicated by the color coding. Additionally, reverse-phase LCMS analysis of the crude product mixture also showed evidence for the presence of the phenazinium ion **15** (along with **12** and/or **14** and **13**; see Fig. S5†). Taken together, these results support the mechanism in which a diiminoquinone intermediate (cf. *E,E*-**9d** and *Z,E*-**9d**) undergoes electrocyclization (and tautomerization) to furnish the dihydrophenazine core.

### 3 Conclusions

Herein, we have demonstrated the contrasting reactivity of benzynes with *trans*- vs. *cis*-azobenzene derivatives. Our observations indicate that when *trans*-azobenzene is employed as a trap for a benzyne, it reacts in a formal  $[2 + 2]$  cycloaddition, followed by electrocyclic ring opening to form

a diiminoquinone intermediate. This can then undergo *E/Z* isomerization and electrocyclic ring closure to furnish dihydrophenazines after a final tautomerization (*cf.* Fig. 3a and b). We then demonstrated, both computationally (*cf.* Fig. 3c) and experimentally (*cf.* Fig. 4), that *cis*-azobenzene is a more competent trap for the benzyne, triggering an alternative reaction process – one that proceeds *via* a formal (3 + 2) cycloaddition event to furnish *N*-aminocarbazole derivatives. A key mechanistic experiment showed that the divergent reaction pathways emanate from the specific geometry of the initial azobenzene derivative. *cis*-Azobenzene was isolated chromatographically and reacted with *o*-benzyne in the dark to afford the aminocarbazole derivative as the only isolable product (*cf.* Fig. 5b).

Additional mechanistic experiments were carried out to rationalize the later stages of the [2 + 2] cascade leading to dihydrophenazines (*cf.* Fig. 3a). The phenanthrene diiminoquinone **12** was synthesized and used to probe the key electrocyclization event furnishing the dihydrophenazine skeleton. Upon heating, a novel net disproportionation process was discovered that led in part to the dihydrophenazine derivative **14**, thereby lending support to our mechanistic rationale for the [2 + 2] reaction cascade between arynes and *trans*-azobenzene (*cf.* Fig. 6). Overall, our data demonstrate two non-convergent reaction pathways, each predetermined by the *trans*- vs. *cis*-geometry of the azobenzene used to engage the benzyne.

## 4 Experimental

### 4.1. General procedure for thermal synthesis of phenazine derivatives from HDDA-generated benzyne and azobenzene derivatives

The polyne precursor (1 equiv.) and the azobenzene derivative (10 equiv.) were combined in a screw-capped culture tube. 1,2-Dichloroethane was added to bring the solution to an initial concentration of the polyne of 0.01 M. The resulting solution was placed in an oil bath maintained at 90 °C for *ca.* 16 h. Subsequently, the reaction mixture was passed through a silica gel plug and eluted with EtOAc. The volatiles were removed under reduced pressure, and the crude residue was purified using MPLC with the elution solvent mixture indicated for each compound.

### 4.2. General procedure for photochemical synthesis of aminocarbazole derivatives from HDDA-generated benzyne and azobenzene derivatives

The azobenzene derivative (3 equiv.) was placed in a quartz glass tube and dissolved in *ca.* 1 mL of benzene. The resulting solution was irradiated at ~254 nm at ambient temperature in a Rayonet reactor fitted with quartz glass mercury vapor lamps. After *ca.* 1 h, the polyne precursor (20 mg, 1 equiv.) was added. This reaction mixture was then irradiated overnight under the same conditions. The reaction mixture was passed through a silica gel plug and eluted with EtOAc. The solvent was removed under reduced pressure, and the crude material was

purified using MPLC with the elution solvent mixture indicated for each compound.

### 4.3. General procedure for photochemical synthesis of aminocarbazole derivatives from Kobayashi generated benzyne and azobenzene derivatives

The azobenzene derivative (3 equiv.) was placed in a quartz glass tube and dissolved in *ca.* 2 mL of acetonitrile. The resulting solution was irradiated at 254 nm at ambient temperature in a Rayonet reactor fitted with quartz glass mercury vapor lamps. After *ca.* 1 h, the *o*-trimethylsilylphenyl triflate ("Kobayashi precursor," 50 mg, 1 equiv.) and cesium fluoride (3 equiv.) were added. The final reaction mixture was then irradiated overnight while being stirred (magnetically) under the same photochemical conditions. The acetonitrile was evaporated under reduced pressure and the residue was partitioned between DCM and water. The organic layer was washed with brine, dried over Na<sub>2</sub>SO<sub>4</sub>, filtered, and concentrated. The residue was purified using MPLC with the elution solvent mixture indicated for each compound.

## Data availability

The data upon which the discussion and conclusions in this manuscript are based can be found in the ESI file.†

## Author contributions

D. S. S. performed all the experimental and computational work; both authors interpreted the data and co-wrote the manuscript.

## Conflicts of interest

There are no conflicts to declare.

## Acknowledgements

This research was supported by the National Science Foundation (CHE-2155042). Some of the NMR spectral data were obtained using an instrument funded by the National Institutes of Health Shared Instrumentation Grant program (S10OD011952). ESI HRMS data were collected at the Analytical Biochemistry Shared Resource Laboratory of Masonic Cancer Center at the University of Minnesota with instrumentation partially funded through a Cancer Center Support Grant (CA-77598). The DFT computational studies were carried out using resources made available through the University of Minnesota Supercomputing Institute (MSI). D. S. S. is a holder of a Wayland E. Noland Excellence Fellowship. X-ray diffraction data were collected with instrumentation made available by the National Science Foundation (MRI-1229400). Dr Victor Young, Jr and Mr Alex Lovstedt performed the X-ray structural analyses.



## Notes and references

- 1 *Modern Aryne Chemistry*, ed. A. Bijū, Wiley-VCH, Verlag GmbH & Co. KGaA Weinheim, 2021.
- 2 *The Chemistry of the Hydrazo, Azo and Azoxy Groups*, ed. S. Patai, John Wiley & Sons, New York, NY, 1997, vol. 2.
- 3 W. Zhang, J. Bu, L. Wang, P. Li and H. Li, Sunlight-mediated [3+2] cycloaddition of azobenzenes with arynes: an approach towards the carbazole skeleton, *Org. Chem. Front.*, 2021, **8**, 5045–5051.
- 4 S. S. Bhojgude, A. Bhunia, R. G. Gonnade and A. T. Bijū, Efficient synthesis of 9-aryldihydrophenanthrenes by a cascade reaction involving arynes and styrenes, *Org. Lett.*, 2014, **16**, 676–679.
- 5 Z. Chen, X. Han, J.-H. Liang, J. Yin, G.-A. Yu and S.-H. Liu, Cycloaddition reactions of benzyne with olefins, *Chin. Chem. Lett.*, 2014, **25**, 1535–1539.
- 6 J. Nakayama, H. Midorikawa and M. Yoshida, Reaction of benzyne with N-benzylideneaniline, *Bull. Chem. Soc. Jpn.*, 1975, **48**, 1063–1064.
- 7 C. W. G. Fishwick, R. C. Gupta and R. C. Storr, The reaction of benzyne with imines, *J. Chem. Soc., Perkin Trans. 1*, 1984, 2827–2829.
- 8 S. Arora, D. S. Sneddon and T. R. Hoye, Reactions of HDDA benzynes with C,N-diarylimines (ArCH = NAr'), *Eur. J. Org. Chem.*, 2020, **2020**, 2379–2383.
- 9 L. L. Fluegel and T. R. Hoye, Hexadehydro-Diels–Alder reaction: benzyne generation via cycloisomerization of tethered triynes, *Chem. Rev.*, 2021, **121**, 2413–2444.
- 10 In a SciFinder search we identified a dozen reviews since 2020 having “phenazine” in the title.
- 11 Y.-X. Che, X.-N. Qi, Q. Lin, H. Yao, W.-J. Qu, B. Shi, Y.-M. Zhang and T.-B. Wei, Design strategies and applications of novel functionalized phenazine derivatives: a review, *J. Mater. Chem. C*, 2022, **10**, 11119–11174.
- 12 J. B. Laursen and J. Nielsen, Phenazine natural products: Biosynthesis, synthetic analogues, and biological activity, *Chem. Rev.*, 2004, **104**, 1663–1685.
- 13 B. Miksa, The phenazine scaffold used as cytotoxic pharmacophore applied in bactericidal, antiparasitic and antitumor agents, *Helv. Chim. Acta*, 2022, **105**, e202200066.
- 14 K. Ujike, S. Kudoh and M. Nakata, First detection of 7,8-diazabicyclo[4.2.0]octa-1,3,5-triene produced from 3,5-cyclohexadiene-1,2-diimine in an argon matrix, *Chem. Phys. Lett.*, 2004, **396**, 288–292.
- 15 K. Ujike, N. Akai, S. Kudoh and M. Nakata, Photoisomerization and photocyclization of 3,5-cyclohexadiene-1,2-diimine and its methyl-substituted derivatives in low-temperature argon matrices, *J. Mol. Struct.*, 2005, **736**, 335–342.
- 16 J. M. Medina, J. L. Mackey, N. K. Garg and K. N. Houk, The role of aryne distortions, steric effects, and charges in regioselectivities of aryne reactions, *J. Am. Chem. Soc.*, 2014, **136**, 15798–15805.
- 17 J.-C. Castillo, J. Quiroga, R. Abonia, J. Rodriguez and Y. Coquerel, The aryne aza-Diels–Alder reaction: flexible syntheses of isoquinolines, *Org. Lett.*, 2015, **17**, 3374–3377.
- 18 D. S. Sneddon and T. R. Hoye, Arylhydrazine trapping of benzynes: mechanistic insights and a route to azoarenes, *Org. Lett.*, 2021, **23**, 3432–3436.
- 19 A. H. Cook and D. G. Jones, cis-Azo-compounds Part IV. Some reactions with diphenylketen, *J. Chem. Soc.*, 1941, 184–187.
- 20 G. O. Schenck and N. Engelhard, Azobenzol-Keten-Addukt, *Angew. Chem.*, 1956, **68**, 71.
- 21 G. O. Schenck, Aufgaben und Möglichkeiten der präparativen Strahlenchemie, *Angew. Chem.*, 1957, **69**, 579–599.
- 22 P. Ruggli and J. Rohner, Über o-Disazo-benzol, *Helv. Chim. Acta*, 1942, **25**, 1533–1542.
- 23 D. J. Tindall, C. Werlé, R. Goddard, P. Philipps, C. Farès and A. Fürstner, Structure and reactivity of half-sandwich Rh(+3) and Ir(+3) carbene complexes. Catalytic metathesis of azobenzene derivatives, *J. Am. Chem. Soc.*, 2018, **140**, 1884–1893.
- 24 F. Xu, X. Xiao and T. R. Hoye, Photochemical hexadehydro-Diels–Alder reaction, *J. Am. Chem. Soc.*, 2017, **139**, 8400–8403.
- 25 Y. Himeshima, T. Sonoda and H. Kobayashi, Fluoride-induced 1,2-elimination of o-(trimethylsilyl)phenyl triflate to benzyne under mild conditions, *Chem. Lett.*, 1983, **12**, 1211–1214.
- 26 For a recent review of Kobayashi benzyne chemistry, see: J. Shi, L. Li and Y. Li, o-Silylaryl triflates: A journey of Kobayashi aryne precursors, *Chem. Rev.*, 2021, **121**, 3892.
- 27 A. Dall'Anese, V. Rosar, L. Cusin, T. Montini, G. Balducci, I. D'Auria, C. Pellicchia, P. Fornasiero, F. Felluga and B. Milani, Palladium-catalyzed ethylene/methyl acrylate copolymerization: Moving from the acenaphthene to the phenanthrene skeleton of  $\alpha$ -diimine ligands, *Organometallics*, 2019, **38**, 3498–3511.
- 28 B. Gao, D. Zhao, X. Li, Y. Cui, R. Duan and X. Pang, Magnesium complexes bearing N,N-bidentate phenanthrene derivatives for the stereoselective ring-opening polymerization of rac-lactides, *RSC Adv.*, 2015, **5**, 440–447.
- 29 X. Jin, S. Li, L. Guo, J. Hua, D.-H. Qu, J. Su, Z. Zhang and H. Tian, Interplay of steric effects and aromaticity reversals to expand the structural/electronic responses of dihydrophenazines, *J. Am. Chem. Soc.*, 2022, **144**, 4883–4896.

